Izvestiya, Atmospheric and Oceanic Physics, Vol. 41, No. 1, 2005, pp. 43–55. Translated from Izvestiya AN. Fizika Atmosfery i Okeana, Vol. 41, No. 1, 2005, pp. 51–65.

Contribution of Natural and Anthropogenic Factors to Long-Term Changes in the Earth's Ozone Layer at the End of the 20th Century

I. G. Dyominov and A. M. Zadorozhny

Novosibirsk State University, ul. Pirogova 2, Novosibirsk, 630090 Russia
e-mail: dyominov@phys.nsu.ru, zadorozh@phys.nsu.ru

Received March 13, 2003; in final form, February 26, 2004

Abstract—The contribution of natural and anthropogenic factors to long-term changes in the ozone layer in the last decades of the 20th century is studied using a numerical two-dimensional ozonosphere model with a self-consistent calculation of photochemical, radiative, dynamic, and microphysical processes. The joint action of anthropogenic emissions of the greenhouse gases CO_2, CH_4, and N_2O and of ozone-destroying chlorine and bromine compounds on the atmosphere is examined. Calculations take into account the stratospheric sulfate aerosol increase caused by the observed growth of the concentration of sulfur-containing gas compounds in the atmosphere and by volcanic eruptions. Numerical experiments have shown that the main cause of the ozone layer depletion since the late 1970s is anthropogenic atmospheric pollution by chlorine- and bromine-containing compounds. The 11-year solar UV flux variations and El Chichon and Pinatubo eruptions also induced substantial ozone changes in that period. Between the solar minimum and maximum, the low- and midlatitude ozone changes induced by solar UV flux variations are comparable in magnitude to changes due to anthropogenic atmospheric pollution. Volcanic eruptions have caused sharper yet shorter-lived disturbances of the ozone layer. It is found that anthropogenic changes in atmospheric chemistry and temperature during the action of volcanic sulfur compounds on the ozone layer significantly extend the period of influence of volcanic eruptions on global ozone. Anthropogenic emissions of greenhouse gases into the atmosphere, mainly carbon dioxide, have a marked effect on the dynamics of the ozone layer. The increase in atmospheric CO_2 reduced global ozone depletion in the 60° S–60° N belt by about 20% in the late 1990s. Changes in the Earth's ozone layer calculated from data on anthropogenic atmospheric pollution, 11-year solar UV flux variations, and volcanic eruptions agree quite well with the global ozone trend observed in the last 25 years of the 20th century.

1. INTRODUCTION

Numerous experimental data [1–5] obtained recently show a tendency of a strong depletion of the Earth's ozone layer starting in the late 1970s. By the end of the 20th century, the total ozone in the atmosphere had decreased by about 5%. In heavily populated northern midlatitudes, the decrease in total ozone (TO) is about 10% in winter and spring and 5% in summer and fall. The maximum ozone depletion (over 60%) is annually observed over Antarctica in spring. During the presence of the ozone hole over Antarctica, the total ozone in its central regions on some days is less than one-third of the background value. The observed ozone changes are induced by ozone decrease in the stratosphere and may be due to anthropogenic emissions of ozone-destroying compounds into the atmosphere as well as to natural factors (solar activity, volcanic eruptions, etc.). It is believed that most of the observed ozone depletion is caused by atmospheric pollution by chlorine- and bromine-containing compounds [1, 6, 7]. However, the relative contribution of natural and anthropogenic factors to observed ozone trends has not yet been determined.

An assessment of the contribution of different sources to observed ozone changes can be made only on the basis of numerical atmospheric models with a self-consistent calculation of a large number of various relations between photochemical, radiative, dynamic, and microphysical processes governing the concentration of ozone in the Earth's atmosphere. The use of such models has shown that the effect of various factors on ozone is not additive; i.e., the response of the ozone layer to the simultaneous action of various disturbances is not a simple sum of the responses to individual disturbances [8–11]. Recent theoretical studies have demonstrated that the response of the Earth's ozone layer to solar activity effects, such as solar proton events and solar UV flux variations, depends strongly on the amount of chlorine compounds and sulfate aerosol in the stratosphere [6, 12–16]. Temperature changes caused by greenhouse-gas atmospheric pollution or volcanic eruptions also influence photochemical processes controlling stratospheric ozone [8, 17–23].

In this paper, the contribution of natural and anthropogenic factors to long-term changes in the ozone layer is studied using a numerical model of the ozonosphere [24–29]. The model takes these effects into account by

means of self-consistent consideration of photochemical, radiative, dynamic, and microphysical processes and inclusion of the maximum possible number of factors that simultaneously influence atmospheric chemistry and temperature. A specific feature of the numerical experiments is a self-consistent simultaneous consideration of the enhancement of atmospheric pollution by the anthropogenic greenhouse gases CO_2, CH_4, and N_2O and by ozone-destroying chlorine and bromine compounds. The model also accounts for the stratospheric sulfate aerosol changes induced by the observed increase of sulfur gas compounds in the atmosphere and by volcanic eruptions.

Stratospheric cooling, which is expected as a result of the greenhouse gas concentration increase in the atmosphere, will influence stratospheric ozone in different ways. First, the stratospheric temperature decrease because of temperature dependence of the rate constants of photochemical reactions [30] will to some extent weaken all catalytic processes of ozone destruction. Hence, stratospheric cooling will lead to ozone increase [22, 23, 29]. Second, stratospheric cooling is expected to cause a more intense formation of polar stratospheric clouds and, consequently, a more rapid ozone destruction initiated by heterogeneous processes on their surface [20, 21]. In this study, we will restrict our analysis to the effect of natural and anthropogenic factors on the ozone layer in middle and low latitudes. All processes important for polar latitudes will also be included in model computations.

2. MODEL DESCRIPTION

To examine the contribution of natural and anthropogenic factors to long-term changes in the Earth's ozone layer in the final decades of the 20th century, we use the Novosibirsk State University (NSU) zonally averaged two-dimensional interactive model of the ozonosphere [24–29]. The model self-consistently calculates the diabatic circulation, temperature and gas composition of the troposphere and stratosphere in the latitudinal region from the North to South Pole, and the distribution of sulfate aerosol particles and particles of polar stratospheric clouds (PSCs) of types I and II.

2.1. Photochemical Block of the Model

Space–time variations of atmospheric trace gases are described in the model by a system of zonally averaged continuity equations [31]

$$\frac{\partial \bar{\mu}_i}{\partial t} + \frac{\partial \Phi_{iz}}{\partial z} + \frac{1}{\cos\varphi}\frac{\partial}{\partial y}(\cos\varphi \Phi_{iy}) = \frac{\bar{P}_i}{\bar{N}} - \bar{l}_i \bar{\mu}_i. \quad (1)$$

Here, $\bar{\mu}_i$ is the zonally averaged mixing ratio of the ith constituent ($\bar{\mu}_i = \bar{n}_i/\bar{N}$, where $\bar{n}_i$ and $\bar{N}$ are the zonally averaged concentration of the ith constituent and the total concentration of molecules in the atmosphere); $\bar{P}_i$ and $\bar{l}_i$ are photochemical sources and sinks of the ith constituent; φ is latitude; and Φ_{iy} and Φ_{iz} are horizontal (along the meridian) and vertical flux components determined by

$$\Phi_{iy} = \bar{v}^* \bar{\mu}_i - K_{yy}\frac{\partial \bar{\mu}_i}{\partial y}, \quad (2)$$

$$\Phi_{iz} = \bar{w}^* \bar{\mu}_i - K_{zz}\frac{\partial \bar{\mu}_i}{\partial z}. \quad (3)$$

In (2) and (3), $\bar{v}^*$ and $\bar{w}^*$ are the horizontal and vertical components of the residual (diabatic) meridional circulation of the atmosphere and K_{yy} and K_{zz} are the horizontal and vertical coefficients of eddy diffusion, respectively.

Space–time variations of trace gases whose lifetimes are small compared to characteristic transport times are described by the nonstationary equation of photochemical equilibrium

$$\frac{\partial \bar{\mu}_i}{\partial t} = \frac{\bar{P}_i}{\bar{N}} - \bar{l}_i \bar{\mu}_i. \quad (4)$$

The model calculates the distribution of 64 trace gases of seven families (O_x, HO_x, NO_y, Cl_y, Br_x, CHO_x, HSO_x) and their source components: O_3, $O(^3P)$, $O(^1D)$, H. OH, HO_2, H_2O_2, H_2O, NO, NO_2, NO_3, N_2O_5, HNO_3, N_2O, CO, CH_4, CH_3, CHO, CH_2O, CH_3O_2, CH_3O_2H, CH_3CO_3, $CH_3CO_3NO_2$, Cl, ClO, OClO, ClOO, HOCl, $ClNO_2$, $ClONO_2$, Cl_2, Cl_2O_2, HCl, CCl_4, CH_3Cl, CH_3CCl_3, $CFCl_3$ (CFC-11), CF_2Cl_2 (CFC-12), $CF_2ClCFCl_2$ (CFC-113), CF_2ClCF_2Cl (CFC-114), CF_2ClCF_3 (CFC-115), CHF_2Cl (HCFC-22), CHF_3Cl_2C (HCFC-123), CH_3CFCl_2 (HCFC-141b), CH_3CF_2Cl (HCFC-142b), Br, BrO, HOBr, HBr, $BrONO_2$, BrCl, CH_3Br, CF_3Br (H-1301), CF_2ClBr (H-1211), CH_3SCH_3, CS, H_2S, OSC, S, SO, SO_2, SO_3, HSO_3, and H_2SO_4. Interactions among gas constituents are governed by 203 photochemical gas-phase reactions, i.e., all presently known reactions important for the photochemistry of the Earth's ozone layer. Reaction rate constants and photodissociation cross sections are taken from [30]. The spectral density of the solar radiation flux in the range 1750–9000 Å is adopted in the model in accordance with [32, 33]. The model also takes into account the sink of gas constituents in heterogeneous reactions on particles of sulfate aerosol

$$N_2O_5 + H_2O(s) \longrightarrow 2HNO_3, \quad (R1)$$

$$ClONO_2 + H_2O(s) \longrightarrow HOCl + HNO_3, \quad (R2)$$

$$BrONO_2 + H_2O(s) \longrightarrow HOBr + HNO_3, \quad (R3)$$

$$ClONO_2 + HCl(s) \longrightarrow Cl_2 + HNO_3, \quad (R4)$$

$$HOCl + HCl(s) \longrightarrow Cl_2 + H_2O, \quad (R5)$$

$$HOBr + HCl(s) \longrightarrow BrCl + H_2O, \quad (R6)$$

and PSCs

$$N_2O_5 + H_2O(s) \longrightarrow 2HNO_3(s), \quad \text{(R7)}$$

$$N_2O_5 + HCl(s) \longrightarrow ClNO_2 + HNO_3(s), \quad \text{(R8)}$$

$$ClONO_2 + H_2O(s) \longrightarrow HOCl + HNO_3(s), \quad \text{(R9)}$$

$$ClONO_2 + HCl(s) \longrightarrow Cl_2 + HNO_3(s), \quad \text{(R10)}$$

$$HOCl + HCl(s) \longrightarrow Cl_2 + H_2O(s), \quad \text{(R11)}$$

$$BrONO_2 + H_2O(s) \longrightarrow HOBr + HNO_3(s), \quad \text{(R12)}$$

$$BrONO_2 + HCl(s) \longrightarrow BrCl + HNO_3(s), \quad \text{(R13)}$$

$$HOBr + HCl(s) \longrightarrow BrCl + H_2O(s). \quad \text{(R14)}$$

Here, (s) indicates a molecule on the surface of a condensed particle. The rates of heterogeneous reactions are calculated using the formula from [34]

$$k = \frac{\gamma S \bar{V}}{4}, \quad (5)$$

where γ is the reaction probability, S is the surface area of condensed particles, and $\bar{V}$ is the mean velocity of gas molecules. Values of γ for heterogeneous reactions R1–R6 on the sulfate aerosol are taken from [30, 35–38]. The model takes into account the fact that the probabilities of reactions R7–R14 strongly depend on the type of polar stratospheric clouds on which they occur. Values of γ for these reactions, in accordance with [30], are taken equal to 0.0003, 0.003, 0.001, 0.1, 0.1, 0, 0, and 0 for PSC I and 0.01, 0.03, 0.3, 0.3, 0.3, 0.3, 0.5, and 0.1 for PSC II, respectively.

By analogy with [25, 39], the model takes into account the washout from the troposphere of the gas constituents HNO_3, H_2O_2, HCl, HBr, CH_2O, CH_3O_2, CH_3O_2H, and H_2SO_4. The distribution of water vapor is calculated by Eq. (1) only in the stratosphere. In the troposphere, the seasonal–latitudinal variations of H_2O concentration are specified in accordance with experimental data on zonally averaged humidity [40, 41]. The seasonal mean values of the vertical and horizontal coefficients of eddy diffusion are taken from [42].

The numerical algorithm used in the model for the system of nonstationary continuity equations (1) and (4) that are rigidly bound by photochemical terms is described in detail in [25]. Advective transfer is taken into account by using the numerical scheme of [43].

2.2. Block for Computation of Condensed Particles

The model considers sulfuric acid hydrate (sulfate aerosol), nitric acid trihydrate (PSC I), and ice (PSC II) particles with radii $0.0064 \le r \le 5.2$, $0.1 \le r \le 25.6$, and $0.5 \le r \le 128$ μm, respectively. Particle size distributions $n_a(r)$ are determined in the model from the corresponding continuity equations

$$\frac{\partial n_a(r)}{\partial t} = P_{nucl} + \left.\frac{\partial n_a(r)}{\partial t}\right|_{cond/evap} + \left.\frac{\partial n_a(t)}{\partial t}\right|_{coag} + \left.\frac{\partial n_a(r)}{\partial t}\right|_{sed} + \left.\frac{\partial n_a(r)}{\partial t}\right|_{transp}. \quad (6)$$

The terms on the right-hand side of (6) describe heterogeneous and homogeneous nucleation, condensation, evaporation, coagulation, sedimentation, washout, and transport by diabatic circulation and eddy diffusion, respectively.

The binary homogeneous nucleation rates are calculated using a classical approach described in detail in [44, 45]. The heterogeneous nucleation rates are calculated according to the method given in [45] and further developed in [46]. Condensation and evaporation are calculated in the model in correspondence with [47, 48]. Brownian coagulation is described with classical relations presented in [49]. Gravitational aerosol sedimentation is determined by analogy with [46]. The transport of condensed particles by eddy diffusion is calculated with the same coefficients, K_{yy} and K_{zz}, as for the gas composition.

For numerical solution of (6), the particle size distribution $n_a(r)$ is replaced by a discrete function N_{ai}:

$$N_{ai} = \frac{1}{\Delta r_i}\int_{r_i}^{r_{i+1}} n_a(r)dr, \quad (7)$$

where i is the number of an interval (a bin) on a grid of partition of particle's radii. For PSC particles, it is assumed that

$$r_{i+1} = 2r_i, \quad \Delta r_i = r_i, \quad r_n = 2^{n-1}r_1. \quad (8)$$

Altogether there are 9 bins for ice particles and 11 bins for sulfuric acid trihydrate. For sulfate aerosol, the entire range of sizes is divided into 30 bins by the rule

$$r_{i+1} = \sqrt[3]{2}r_i, \ \Delta r_i = (\sqrt[3]{2} - 1)r_i, \ r_n = \sqrt[3]{2^{n-1}}r_1. \quad (8')$$

Thus, the total number of bins for PSC I, PSC II, and sulfate aerosol particles is 50. Then, the solution of the continuity equations for particle size distributions (6) reduces to the solution of a system of 50 difference equations. This system of equations is solved by a numerical semiexplicit scheme [50]. The solution is carried out using a relaxation method. Under relatively arbitrary initial conditions, the solution of the system converges in about two model years.

2.3. Radiative Block of the Model

The temperature stratification of the atmosphere is determined by the heat balance equation

$$Q(z, y, \bar{T}(z, y)) = 0, \quad (9)$$

where the atmospheric heating is determined by the relation from [51, 52]

$$Q(z, y, \bar{T}) = \frac{\partial \bar{T}(z, y)}{\partial t} = \frac{1}{c_p \rho(z, y)} \times (\varepsilon_{VT}(z, y) + \varepsilon_{HT}(z, y) + \varepsilon_S(z, y) + \varepsilon_{IR}(z, y)) = 0. \quad (10)$$

Here, $\bar{T}$ is the zonally averaged temperature; ε_{VT} and ε_{HT} are the vertical and horizontal heat fluxes due to convection and turbulent heat exchange, respectively; ε_S and ε_{IR} are the heat fluxes due to solar and thermal radiation transfer, respectively; c_p is the heat capacity at constant pressure; and ρ is the atmospheric density. Expressions for heat fluxes can be found in [51, 52].

Calculation of the heat fluxes due to solar and thermal radiation transfer takes into account radiative fluxes in three spectral ranges: ultraviolet and visible (0.175–0.9 μm), near infrared (0.9–4.0 μm), and infrared (>4 μm). The radiative fluxes in the UV and visible part of the spectrum are computed by taking into account scattering on air molecules and aerosol particles; reflection from clouds and the Earth's surface; and absorption by O_2, O_3, and NO_2. In the near infrared, absorption by water vapor in the 0.94-, 1.1-, 1.38-, 1.87-, 2.7-, and 3.2-μm bands and by carbon dioxide in the 2.0- and 2.7-μm bands, as well as by aerosol and clouds, is considered. In the infrared range, absorption by CO_2, O_3, H_2O, CH_4, N_2O, $CFCl_3$, and CF_2Cl_2 is taken into consideration. The fine spectral structure of these constituents is taken into account in the absorption bands centered at 15, 9.6, 6.3, 7.6, (4.5, 7.78, 8.57, and 17), (9.22 and 11.82), and (8.68, 9.13, and 10.93) μm, respectively. In addition, the model takes into account absorption of heat radiation by aerosol particles and clouds and absorption in rotational bands of water vapor.

The algorithm of reconstruction of the equilibrium distribution of temperature from Eq. (9) is described in [52].

2.4. Dynamic Block of the Model

Dynamic processes in the atmosphere are represented in the model by the residual (diabatic) meridional circulation [31, 53] and eddy diffusion. The residual circulation is described by the system of zonally averaged equations of horizontal motion, thermodynamic energy equation, and the thermal-wind equation

$$\frac{\partial \bar{u}}{\partial t} - \bar{f}\bar{v}^* + \frac{\partial \bar{u}}{\partial z}\bar{w}^* = -K_R\bar{u}, \quad (11)$$

$$\frac{\partial \bar{T}}{\partial t} + \frac{\partial \bar{T}}{\partial y}\bar{v}^* + S\bar{w}^* = Q_d - G, \quad (12)$$

$$f\frac{\partial \bar{u}}{\partial z} = -\frac{R}{H}\frac{\partial \bar{T}}{\partial y}. \quad (13)$$

Here, $\bar{u}$ is the velocity of zonal flow, R is the gas constant, H is the height of a homogeneous atmosphere, K_R is the coefficient of Rayleigh friction, Q_d is the rate of diabatic heating (cooling), G are heat fluxes due to eddy diffusion, $S = \frac{H}{R}N_S^2 + \frac{\partial \bar{T}}{\partial z}$, and N_S is the Brunt–Väisälä frequency. The parameters $\bar{f}$ and f are determined according to [54] by the relations

$$\bar{f} = l - \frac{\partial \bar{u}}{\partial y} + \frac{\bar{u}\tan\varphi}{a}, \quad (14)$$

$$f = l + \frac{2\bar{u}\tan\varphi}{a}, \quad (15)$$

where a is the radius of the Earth, $l = 2\Omega\sin\varphi$ is the Coriolis parameter, and Ω is the angular velocity of the Earth's rotation. The eddy heat fluxes are given by

$$G = -\frac{1}{\cos\varphi}\frac{\partial}{\partial y}\left(\cos\varphi K_{yy}\frac{\partial \bar{T}}{\partial y}\right) - \frac{1}{\rho}\frac{\partial}{\partial z}\left(\rho K_{zz}\left(\frac{\partial \bar{T}}{\partial z} + \frac{g}{c_p}\right)\right). \quad (16)$$

To calculate the residual meridional circulation, we introduce a stream function $\bar{\psi}^*$ given by

$$\frac{\partial \bar{\psi}^*}{\partial y} = \bar{w}^*\cos\varphi, \quad (17)$$

$$\frac{\partial \bar{\psi}^*}{\partial z} - \frac{\bar{\psi}^*}{H} = -\bar{v}^*\cos\varphi. \quad (18)$$

Using (11), (12), and (13), one can obtain the following equation for $\bar{\psi}^*$:

$$A_{zz}\frac{\partial^2 \bar{\psi}^*}{\partial z^2} + A_{zy}\frac{\partial^2 \bar{\psi}^*}{\partial z \partial y} + A_{yy}\frac{\partial^2 \bar{\psi}^*}{\partial y^2} + A_z\frac{\partial \bar{\psi}^*}{\partial z} + A_y\frac{\partial^2 \bar{\psi}^*}{\partial y} = A_F\cos\varphi. \quad (19)$$

Expressions for the coefficients A_{zz}, A_{zy}, A_{yy}, A_z, A_y, and A_F are given in [31].

Differential equation (19) is solved by the well-known integral-interpolation method [50]. Boundary conditions for this equation are set as follows: at the poles, $\bar{\psi}^* = 0$; at the upper boundary, we set $\frac{\partial \bar{\psi}^*}{\partial z} = 0$; and at the lower boundary, we specify the values of $\bar{\psi}^*$ taken from [55].

2.5. Computations of the Background State of the Atmosphere

The model is calculated on a grid with a horizontal resolution of 5° in latitude in the domain from the North to South Pole and a vertical resolution of 2 km for alti-

tudes from the Earth's surface to 50 km. Nonstationary continuity equations for gas constituents (1) and continuity equations for particle size distributions (6) are solved with a time step of 24 h. The diurnal variation of photodissociation rates is recalculated every tenth model day to determine the daily mean photochemical sources and sinks $\bar{P}_i$ and $\bar{l}_i$. At each time step, the atmospheric temperature is calculated from heat balance equation (10) and the meridional circulation is derived from Eqs. (11)–(13) and (16). The results are used at a given step to solve the system of continuity equations for the gas and aerosol composition of the atmosphere. Thus, the self-consistency of the solution of the system of original equations is achieved.

The initial state of a weakly polluted atmosphere corresponding to 1975 is calculated by the relaxation method. Under initial conditions specified almost arbitrarily, the self-consistent solution of the system of original equations converges in ~8 model years. Time dependences of percentage changes in total ozone for 1975–2000 are given below. The computation was carried out relative to the values at the end of 1979, when solar activity was at an average level.

The seasonal–latitudinal distribution of total ozone in the atmosphere and the altitude–latitude distribution of atmospheric temperature for 1979 are shown in Fig. 1. It is seen that the model adequately reflects the observed features in the distribution of given parameters. The NSU ozonosphere model in different stages of its development has participated twice in international 2-D model intercomparisons [27, 56]. The intercomparisons have shown that the NSU model is as successful as the best models of a given class in considering physicochemical processes and modeling the observed space–time variations of the ozone layer.

3. CAUSES OF LONG-TERM VARIATIONS OF THE OZONE LAYER

This paper considers three causes of long-term variations of the ozone layer: anthropogenic atmospheric pollution, 11-year solar cycle UV variations, and volcanic eruptions. Solar proton events (SPEs) and galactic cosmic rays are disregarded in computations. A substantial ozone decrease of about 20–25% was observed only in the upper stratosphere during the October 1989 SPEs (the strongest SPEs ever recorded in the entire period from 1975 to 2000) [57]. Model computations predict that the total ozone during these gigantic SPEs would change by a mere 1% and only at polar latitudes [6, 16].

Model computations take into account anthropogenic atmospheric pollution by the greenhouse gases CO_2, CH_4, and N_2O and by ozone-destroying chlorine compounds (CFC-11, CFC-12, CFC-113, CFC-114, CFC-115, HCFC-22, HCFC-123, HCFC-141b, HCFC-142b, CCl_4, CH_3Cl, CH_3CCl_3) and bromine compounds (H-1211, H-1301, CH_3Br). Scenarios of anthropogenic trends of these gas constituents for the period from 1975 to 2000 are taken from the WMO report [1]. These scenarios are based on observations and their extrapolation to the future with predicted anthropogenic emissions into the atmosphere in accordance with adopted international agreements. Pollutant concentrations at the ground (Table 12-2 in [1]), varying according to the adopted scenarios, are used as the lower boundary conditions in computations with a nonstationary model.

The solar UV spectrum variation between solar minimum and maximum was modeled on the basis of [58] and is given in the table. This variability of the Earth's incoming radiation is based on experimental data [59]. It is accepted in the model that the solar UV radiation flux varies in time by a sine law with an 11-year period.

According to [60], the total annual mean amount of sulfate aerosol in the stratosphere in 1975 was about 300 kt. Boundary conditions for sulfur gas compounds at the Earth's surface were chosen in the model such that the calculated amount of sulfate aerosol matched this value. In addition, it was accepted that the increase in sulfur gas compounds in the stratosphere should correspond to an observed increase of 12 kt per year in the total annual mean amount of sulfate aerosol [61]. In this case, the amount of sulfate aerosol in the stratosphere increases from 300 kt in 1975 to 600 kt in 2000. The model also takes into account atmospheric emissions of sulfur compounds from the eruptions of El Chichon (April 4, 1982, Mexico) and Mount Pinatubo (June 15, 1991, Philippines), which were the strongest during the given period. In accordance with available data [62–66], the model considers that, in the 5° S–15° N latitude range, sulfate clouds formed during a few days after the eruptions of El Chichon and Mount Pinatubo at altitudes of 19–26 and 16–34 km, respectively. The total mass of sulfur compounds in the clouds after the eruptions of El Chichon and Mount Pinatubo is taken equal to 8.5 and 20 Mt, respectively. In accordance with the EXP2 scenario [67], the model treats the clouds as containing 65% of SO_2 and 35% of sulfate aerosol.

The model does not consider finely dispersed volcanic ash particles formed immediately during the eruption because they are removed rapidly from the stratosphere as a result of intense coagulation and are unimportant in long-term stratospheric variations [49].

4. RESULTS AND DISCUSSION

Figure 2 shows the calculated total ozone changes in the 60° S–60° N latitudinal belt induced by 11-year solar UV flux variations from 1975 to 2000 and by the El Chichon and Mount Pinatubo eruptions. Changes in the chemical composition of the atmosphere due to anthropogenic pollution were disregarded in these computations. The results show an increase in global ozone of ~1.15% between the solar minimum and maximum. A more detailed description of the effect of 11-year solar UV variations on the ozone layer is given

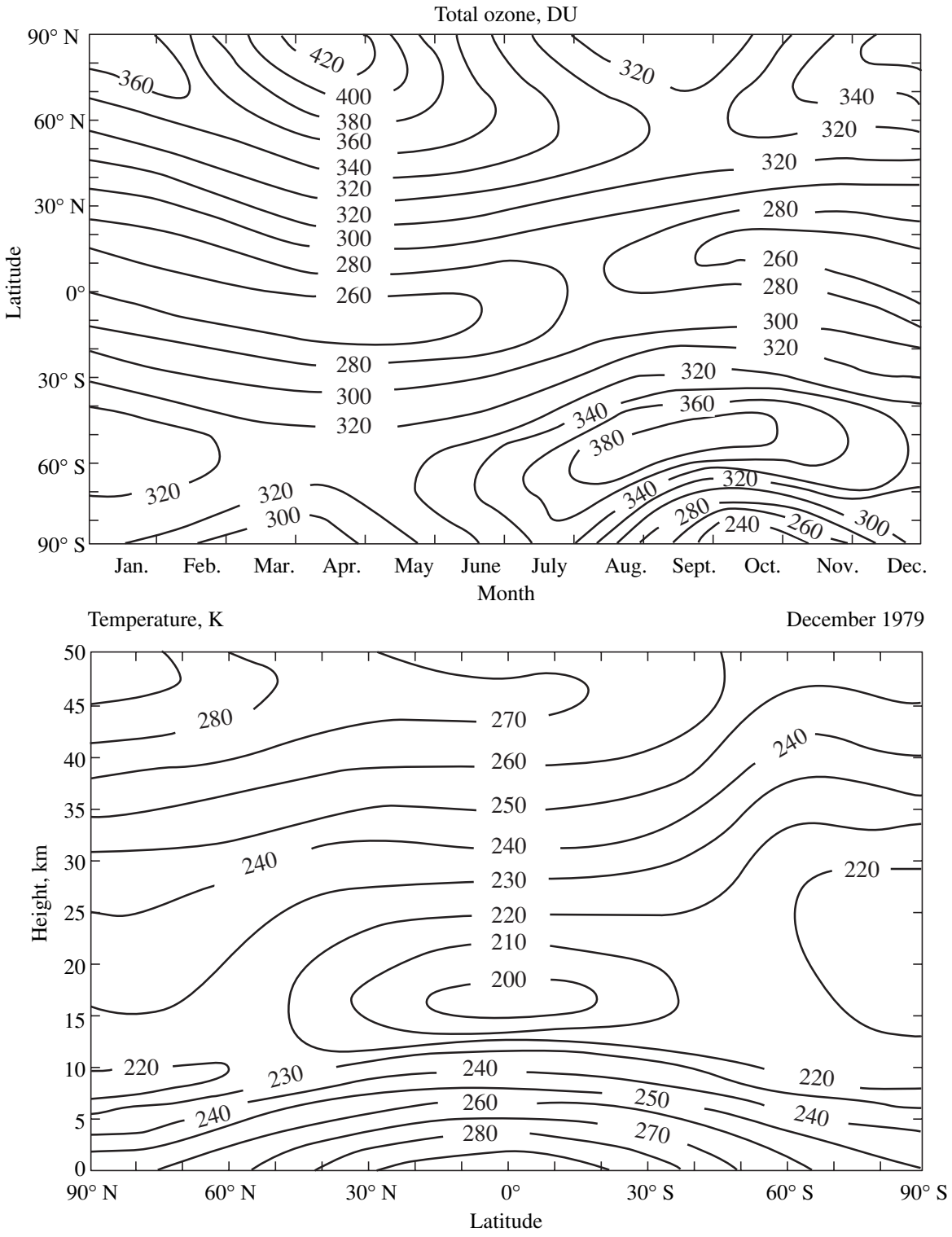

Fig. 1. Seasonal–latitudinal distribution of total ozone and altitude–latitude distribution of atmospheric temperature for 1979.

in [29]. Maximum global ozone decreases after the volcanic eruptions were ~1.6% and ~2.7% for El Chichon and Mount Pinatubo, respectively. From Fig. 2, it can be seen that global ozone changes induced by 11-year solar cycle UV variations are comparable to changes caused by volcanic eruptions. The period of the global ozone disturbances induced by volcanic eruptions is not greater than about two or three years.

Model computations have shown that the ozone depletion induced by a volcanic eruption is due to stratospheric warming and a change in the distribution of ozone-destroying gas constituents in the stratosphere. The change in gas composition is initiated by heterogeneous reactions on the surface of sulfate aerosol particles formed from volcanic sulfur compounds injected into the stratosphere. The relative role of the radiative and heterogeneous photochemical mechanisms of the influence of volcanic eruptions on the ozone layer is shown in Fig. 3 by example of the Mount Pinatubo eruption. Changes in the ozone layer due to a volcanic eruption in an anthropogenically undisturbed atmosphere were calculated using three scenarios in which (1) heterogeneous processes on sulfate particles of volcanic origin were disregarded (illustration of a "radiative" mechanism); (2) radiative processes on these particles were neglected (illustration of a "heterogeneous photochemical" mechanism), and (3) all processes were considered.

The temperature of the stratosphere after volcanic eruptions strongly increases due to intense absorption of heat radiation by sulfate aerosol particles whose surface area density after volcanic eruptions increases drastically. In turn, the stratospheric temperature increase, due to temperature dependences of the rate constants of photochemical reactions [30], to some extent enhances all catalytic processes of ozone destruction. As a result, the stratospheric warming leads to ozone decrease. This mechanism of the influence of temperature changes on ozone is most efficient at altitudes above 25–30 km. It should be noted that temperature feedbacks play an important role [10]. From Fig. 3, it is seen that the temperature mechanism of atmospheric ozone depletion is initiated by volcanic eruptions and exists just over a year after them, with a maximum effect in the second half of the year.

Computations have shown that the global ozone depletion after the El Chichon and Mount Pinatubo eruptions induced by a disturbance of stratospheric chemistry is initiated by heterogeneous reactions R1–R6 on the surface of sulfate aerosol particles. These reactions affect ozone in two ways. First, they substantially decrease the amount of ozone-active nitric compounds NO_y due to the conversion of N_2O_5, $ClONO_2$, and $BrONO_2$ into passive nitric acid HNO_3. The NO_y decrease leads, on the one hand, to a reduction in ozone losses in the nitric catalytic cycle and, on the other hand, to a redistribution of chlorine and bromine constituents, which, in turn, increases ozone losses in the chlorine and bromine cycles of ozone destruction. The second effect is more substantial, so the NO_y decrease induced by heterogeneous hydration of N_2O_5, $ClONO_2$, and $BrONO_2$ results in additional ozone losses in the stratosphere. Second, these heterogeneous reactions transform chemically inert $ClONO_2$, $BrONO_2$, and HCl into active ozone-destroying compounds HOCl, HOBr, Cl_2, and BrCl, which significantly increases ozone losses in chlorine and bromine catalytic cycles of ozone destruction and, consequently, also leads to an additional depletion of the ozone layer.

Solar UV spectrum variation in the 11-yr solar cycle [58, 59] used in the model

Wavelength, nm	Change, %
150–159	20
159–170	14
170–185	10
185–190	9
190–200	7.6
200–208	6.6
208–266	3
266–270	0.6
270–277	2
277–282	6
282–303	0.8

The heterogeneous photochemical mechanism of the effect of volcanic eruptions on the ozone layer begins to act only during the second year following the eruption and lasts more than a year; for the Pinatubo eruption slightly above two years (Fig. 3). The maximum depletion of the ozone layer in this case occurs in about the middle of the second year after the eruption. Photochemical processes produced by heterogeneous reactions on sulfate aerosol affect the ozone depletion more strongly than radiative processes. In the case of the Mount Pinatubo eruption, the decrease in global ozone induced by the photochemical mechanism is nearly twice that initiated by the radiative mechanism.

The time lag between the peaks of the radiative and heterogeneous photochemical mechanisms of the effect of volcanic eruptions on global ozone (see Fig. 3) is explained by the fact that the first mechanism is most efficient in the equatorial region in the upper stratosphere, while the second is most active in higher latitudes at smaller heights. The El Chichon and Mount Pinatubo eruptions both occurred near the equator. Therefore, it is logical that the radiative mechanism in a given case began to act earlier. The characteristic time of horizontal mixing in the stratosphere is more than a year. Therefore, this is about the same time taken for the photochemical products of a volcanic cloud to spread across the entire stratosphere and for a second (photochemical) mechanism to begin to act. Computations have shown that, in a "clean" atmosphere, global ozone changes induced by volcanic eruptions are actually equal to the sum of changes initiated by radiative factors and heterogeneous photochemical processes. This explains the double-peaked response of global ozone to volcanic eruptions, which was obtained in the numerical experiments and is clearly seen in Figs. 2 and 3.

Figure 4 shows the computations of the global ozone change in the 60° S–60° N belt induced by anthropogenic atmospheric pollution alone and by the joint action

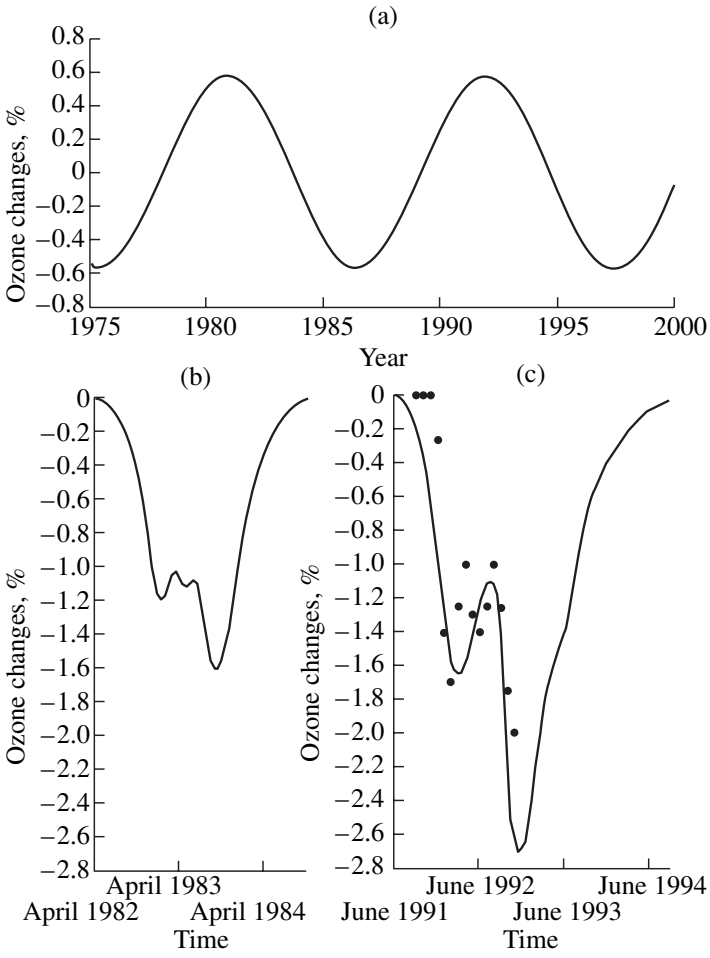

Fig. 2. Calculated changes in monthly mean global ozone in the 60° S–60° N latitudinal belt due to (a) 11-yr solar cycle UV variations, (b) the El Chichon eruption, and (c) the Pinatubo eruption. Observational data after the Pinatubo eruption [68] are shown by dots.

of different sources of long-term ozone variations considered in the model. The solid curve in Fig. 4 corresponds to ozone changes due to anthropogenic emissions of CO_2, CH_4, N_2O, and chlorine and bromine compounds. It is seen that anthropogenic pollution of the atmosphere induces a global ozone depletion in 1997 of about 4.6% compared to 1975. This means that the rate of depletion of the ozone layer due to anthropogenic pollution during that period was on average ~2.1% per decade. This value matches the global ozone change induced by solar UV flux variations in switching from the solar minimum to maximum or vice versa.

The dashed curve in Fig. 4 shows the calculated changes in global ozone due to the simultaneous effect of anthropogenic pollution and 11-year solar UV flux variations. The solid line with points represents global ozone changes induced by the simultaneous effect of all the factors considered in the model: anthropogenic pollution of the atmosphere, 11-year solar UV flux variations, and the El Chichon and Mount Pinatubo eruptions. It is clear that the major contribution to the calculated trend of global ozone is made by anthropogenic pollution of the atmosphere. However, 11-year solar UV flux variations and the El Chichon and Mount Pinatubo eruptions both induced significant changes in global ozone during a given period. Thus, the global ozone increase due to the enhancement of the solar UV radiation flux in 1976–1980 and 1986–1991 compensated the ozone depletion induced by anthropogenic atmospheric pollution and even resulted in a small ozone increase during these periods. This effect combined with the El Chichon eruption happened during the fall of solar activity is the cause of the relatively weak ozone changes between 1983 and 1991. The ozone depletion induced by the Mount Pinatubo eruption near the period of maximum solar activity is more than twice the global ozone increase due to solar UV radiation growth. This caused an extremely low ozone content in 1993.

It is important to note that anthropogenic changes in atmospheric chemical composition, temperature, and dynamics during the impact of volcanic sulfur com-

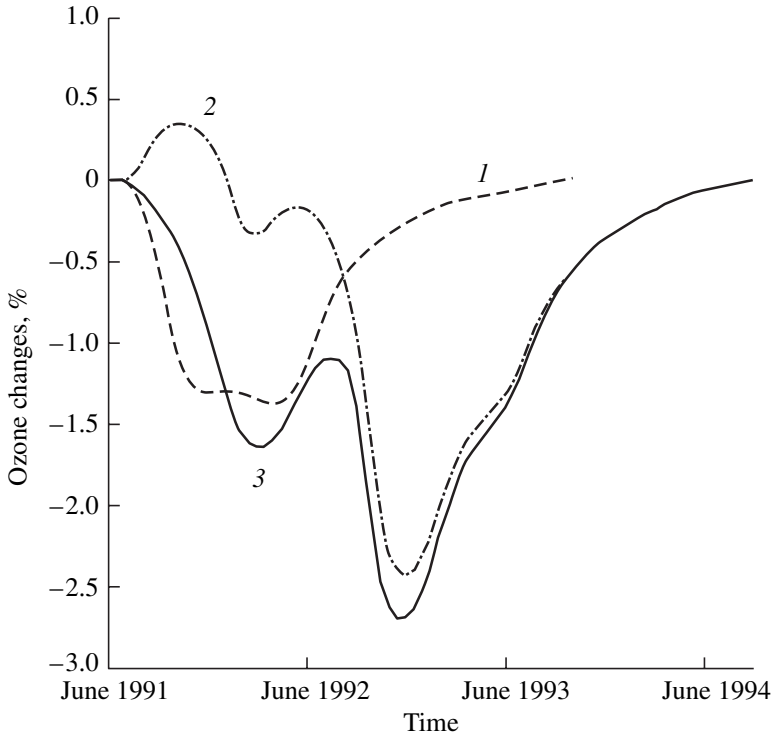

Fig. 3. Contributions of the radiative and heterogeneous photochemical mechanisms of the effect of volcanic eruptions on the ozone layer to monthly mean global ozone changes in the 60° S–60° N latitudinal belt induced by the Pinatubo eruption: (*1*) effect through temperature, (*2*) effect through photochemistry, and (*3*) total effect.

pounds on the ozone layer significantly extended the period of the effect of volcanic eruptions on global ozone (cf. Fig. 2 and Fig. 4). In the case of the Mount Pinatubo eruption, this period increased from about three to five years. The numerical experiments performed have demonstrated that the increase in the duration of the volcanic effect on the ozone layer is caused by two factors operating in that period: anthropogenic change in stratospheric chemistry and anthropogenic temperature change. The contributions from both factors are nearly the same. As in a "clean" atmosphere, heterogeneous processes on the surface of sulfate aerosol and the temperature dependence of stratospheric ozone play a critical role in a polluted atmosphere during the period of the volcanic effect on the ozone layer.

Anthropogenic pollution of the atmosphere by greenhouse gases leads to some stratospheric cooling in the period of influence of volcanic eruptions on the ozone layer. During the first year, when volcanic eruptions influence the ozone layer through a radiative mechanism, this cooling somewhat compensates ozone depletion induced by the temperature rise due to volcanic warming of the stratosphere. However, when the heterogeneous photochemical mechanism begins to act, anthropogenic stratospheric cooling against the background of anthropogenic increases in chlorine and bromine ozone-destroying compounds and the anthropogenic increase in sulfate aerosol intensifies heterogeneous reactions on the surface of these. This enhances the effect of global ozone depletion by volcanic ejection, which is weaker in a "clean" atmosphere. Analysis of the computations shows that the influence of temperature on the ozone layer through temperature dependences of the rate constants of gas-phase reactions is much weaker. As a result, the duration of the volcanic disturbance of the ozone layer increases. It should be noted that this effect is a manifestation of the nonlinear interaction of different factors that disturb the atmosphere and lead to a modification of the ozone layer. In a cooler stratosphere (due to an anthropogenic greenhouse gas increase in the atmosphere) with a high concentration of chlorine and bromine compounds, volcanic eruptions destroy the ozone layer more intensely.

The main contribution to stratospheric cooling due to anthropogenic greenhouse gas emissions and, hence, to the greenhouse effect on the ozone layer described above comes from carbon dioxide. The curve with squares in Fig. 4 shows the calculated global ozone changes in the 60° S–60° N belt induced by all of the anthropogenic emissions except CO_2. The difference of this curve from the solid line in Fig. 4 illustrates the influence of CO_2 emissions on the long-term ozone variations due to anthropogenic atmospheric pollution. It can be seen that the observed carbon dioxide increase at the end of the 20th century substantially reduced the degree of influence of anthropogenic chlorine and bro-

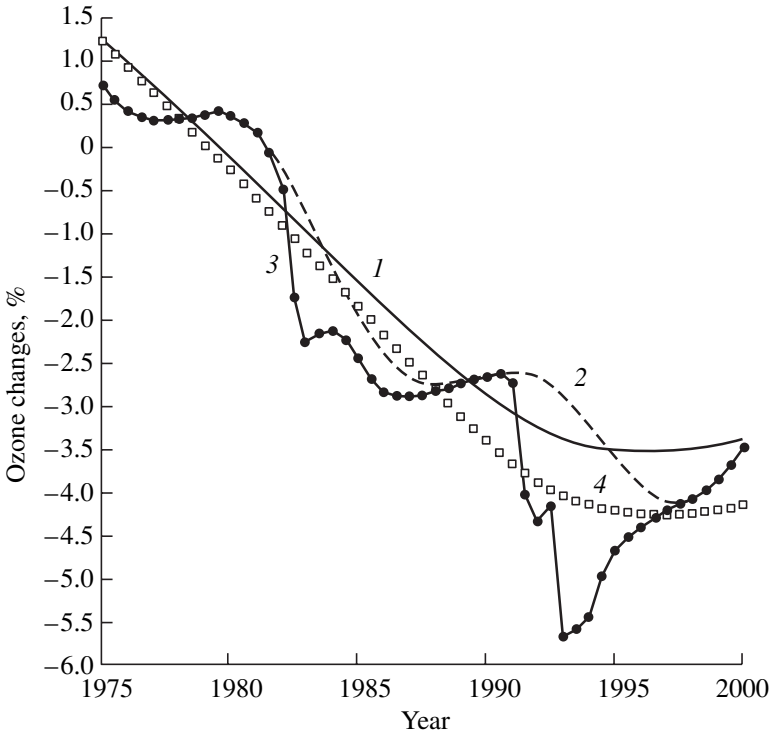

Fig. 4. Calculated half-year averaged changes in global ozone in the 60° S–60° N latitude belt due to anthropogenic pollution (with and without CO_2 emissions), 11-year solar UV flux variations, and volcanic eruptions: (*1*) pollution, (*2*) pollution plus UV, (*3*) pollution plus UV plus volcanic eruptions, (*4*) only pollution without CO_2.

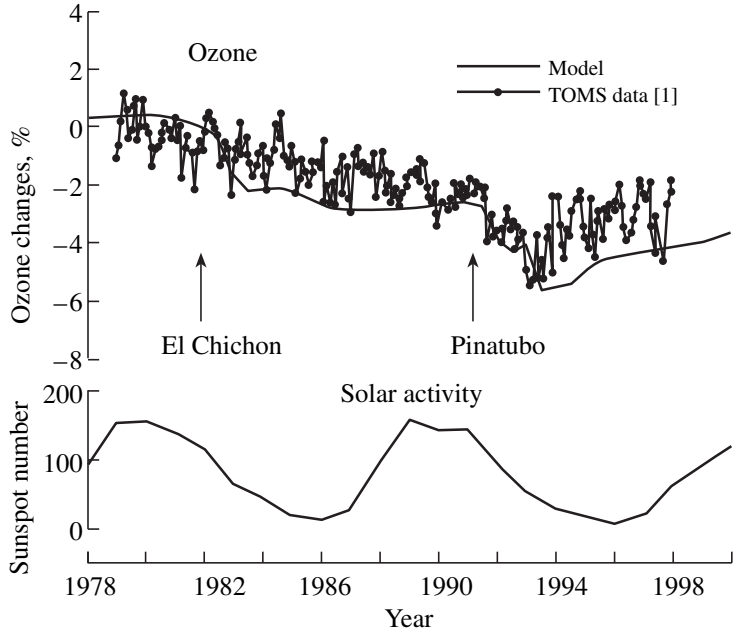

Fig. 5. Observed changes in monthly mean global ozone in the 60° S–60° N latitudinal belt [1] and calculated half-year averaged changes induced by the simultaneous effect of anthropogenic pollution, 11-year solar UV flux variations, and volcanic eruptions. Vertical arrows show the time of the El Chichon and Pinatubo eruptions. The time variation of the sunspot number is shown at the bottom.

mine compounds on the ozone layer in low and middle latitudes. Thus, a reduction in global ozone depletion in a given latitude zone due to the atmospheric CO_2 increase in the late 1990s was about 20%.

Figure 5 compares the model global ozone changes in the 60° S–60° N latitudinal belt calculated with consideration of anthropogenic atmospheric pollution, volcanic eruptions, and 11-year solar cycle UV variations

with TOMS-derived changes. Comparison shows a good agreement of the model computations with measurements. This is due mainly to a self-consistent simultaneous calculation of various sources of long-term atmospheric changes. In particular, the model computations take into account anthropogenic atmospheric emissions of greenhouse gases, mainly of CO_2, which diminish, as was found above, the degree of influence of chlorine and bromine compounds on the ozone layer in low and middle latitudes. The inclusion of this factor has considerably improved the agreement of the computations with observations.

In previous studies [6, 7], which used anthropogenic atmospheric pollution scenarios similar to those accepted in this paper, it was also found that consideration of solar UV flux variations and volcanic eruptions, in addition to anthropogenic emissions of halogen-containing compounds, significantly improved the agreement of computations with observations. The main distinctive features of the present study are the inclusion of the observed growth of greenhouse gases in the atmosphere and a self-consistent calculation of sulfate compounds. These specific features of the study have made it possible to determine the influence of CO_2 emissions on ozone concentration in low and middle latitudes. The influence of CO_2 was most pronounced in the late 1990s and seems to be the main cause of a weaker depletion of the ozone layer compared to the results of [6, 7]. Thus, the calculated global ozone decrease in the 65° S–65° N latitudinal belt in mid-1994 was ~6.5% in [6] and ~5.5% in this paper (Figs. 4, 5).

5. CONCLUSIONS

Numerical experiments have shown that anthropogenic pollution of the atmosphere by chlorine and bromine compounds is the main cause of the ozone depletion observed during the final decades of the 20th century. However, 11-year solar UV flux variations and the El Chichon and Mount Pinatubo eruptions both induced significant changes in global ozone in that period. It is found that anthropogenic emissions of greenhouse gases into the atmosphere, mainly carbon dioxide emissions, have a marked effect on the dynamics of ozone changes induced by other anthropogenic and natural factors. Analysis of the model results uncovered and explained the extension of the period of influence of volcanic eruptions on the ozone layer in the atmosphere anthropogenically disturbed by greenhouse and ozone-destroying gases. This effect is a manifestation of the nonlinear interaction of various factors disturbing the ozone layer. It was also found that the increased amount of ozone in the stratosphere induced by the stratospheric cooling due to carbon dioxide increase in the atmosphere partly compensated the depletion of the ozone layer in low and middle latitudes in the late 20th century due to anthropogenic emissions of chlorine and bromine compounds.

ACKNOWLEDGMENTS

This work was in part supported by the Russian Ministry of Education, grant no. E00-12.0-69, and the Russian Foundation for Basic Research, project nos. 00-05-65187 and 03-05-64642.

REFERENCES

1. *Scientific Assessment of Ozone Depletion: 1998*, WMO Global Ozone Research and Monitoring Project Report No. 44 (Geneva, 1999).
2. R. D. Bojkov, L. Bishop, and V. E. Fioletov, "Total Ozone Trends from Quality Controlled Ground-Based Data (1964–1994)," J. Geophys. Res. D **100**, 25867–25876 (1995).
3. S. M. Hollandsworth, R. D. McPeters, L. E. Flynn, *et al.*, "Ozone Trends Deduced from Combined Nimbus 7 SBUV and NOAA II SBUV/2 Data," Geophys. Rev. Lett. **22**, 905–908 (1995).
4. R. D. McPeters and G. L. Labow, "An Assessment of the Accuracy of 14.5 Year of Nimbus 7 TOMS Version 7 Ozone Data by Comparison with the Dobson Network," Geophys. Rev. Lett. **23**, 3695–3698 (1996).
5. D. M. Cunnold, H. Wang, W. Chu, and L. Froidevaux, "Comparison between SAGE II and MLS Ozone Measurements and Aliasing of SAGE II Ozone Trends in the Lower Stratosphere," J. Geophys. Res. D **101**, 10061–10076 (1996).
6. C. H. Jackman, E. L. Fleming, S. Chandra, *et al.*, "Past, Present, and Future Modeled Ozone Trends with Comparison to Observed Trends," J. Geophys. Res. D **101**, 28753–28767 (1996).
7. S. Solomon, "Stratospheric Ozone Depletion: A Review of Concepts and History," Rev. Geophys. **37**, 275–316 (1999).
8. L. B. Callis, M. Natarajan, and R. E. Boughner, "On the Relationship between the Greenhouse Effect, Atmospheric Photochemistry, and Species Distribution," J. Geophys. Res. C **88**, 1401–1426 (1983).
9. G. Brasseur, A. De Rudder, and C. Tricot, "Stratospheric Response to Chemical Perturbations," J. Atmos. Chem. **3**, 261–288 (1985).
10. I. G. Dyominov and E. I. Ginzburg, "Study of Ozone and Temperature Variations in the Middle Atmosphere Due to Anthropogenic Disturbances," Izv. Akad. Nauk SSSR, Fiz. Atmos. Okeana **25**, 563–572 (1989).
11. I. G. Dyominov and A. M. Zadorozhny, "Study of Ozone and Temperature Variations in the Troposphere and Stratosphere Due to Anthropogenic Perturbations," in *Non-CO_2 Greenhouse Gases: Scientific Understanding, Control and Implementation*, Ed. by J. van Ham, A. P. M. Baede, L. A. Meyer, and R. Ybema (Kluwer, Dordrecht, 2000).
12. I. G. Dyominov, "Effect of Solar Activity on an Anthropogenically Disturbed Atmosphere," in *Study of Atmospheric Ozone (Ozon-90)* (Gidrometeoizdat, Moscow, 1992), pp. 98–104 [in Russian].
13. G. Brasseur, "The Response of the Middle Atmosphere to Long-Term and Short-Term Solar Variability: A Two-Dimensional Model," J. Geophys. Res. D **98**, 23079–23090 (1993).

14. S. Solomon, R. W. Portmann, R. R. Garcia, *et al.*, "The Role of Aerosol Variations in Anthropogenic Ozone Depletion at Northern Midlatitudes," J. Geophys. Res. D **101**, 6713–6728 (1996).
15. E. L. Fleming, S. Chandra, C. H. Jackman, *et al.*, "The Middle Atmospheric Response to Short and Long Term Solar UV Variations: Analysis of Observations and 2D Model Results," J. Atmos. Terr. Phys. **57**, 333–365 (1995).
16. C. H. Jackman, E. L. Fleming, and F. M. Vitt, "Influence of Extremely Large Solar Proton Events in a Changing Stratosphere," J. Geophys. Res. D **105**, 11659–11670 (2000).
17. I. L. Karol', A. A. Kisilev, and V. A. Frol'kis, "Modeling the Influence of the Expected Variations in Methane and Carbon Monoxide Emissions on the Composition of the Global Atmosphere in the Presence of a Greenhouse Effect," Izv. Akad. Nauk, Fiz. Atmos. Okeana **29**, 621–625 (1993).
18. G. Pitari and G. Visconti, "Possible Effects of CO_2 Increase on the High-Speed Civil Transport Impact on Ozone," J. Geophys. Res. D **99**, 16879–16896 (1994).
19. D. E. Kinnison, K. E. Grant, P. S. Connell, *et al.*, "The Chemical and Radiative Effects of the Mount Pinatubo Eruption," J. Geophys. Res. D **99**, 25705–25731 (1994).
20. M. Y. Danilin, N.-D. Sze, M. K. W. Ko, *et al.*, "Stratospheric Cooling and Arctic Ozone Recovery," Geophys. Rev. Lett. **25**, 2141–2144 (1998).
21. D. T. Shindell, D. Rind, and P. Lonergan, "Increases in Polar Stratospheric Ozone Losses and Delayed Recovery Owing to Increasing Greenhouse Gas Concentrations," Nature **392** (6676), 589–592 (1998).
22. L. K. Randeniya, P. F. Vohralik, and I. C. Plumb, "Stratospheric Ozone Depletion at Northern Mid Latitudes in the 21st Century: The Importance of Future Concentrations of Greenhouse Gases Nitrous Oxide and Methane," Geophys. Rev. Lett. **29** (4), 10-1–10-4 (2002).
23. M. P. Chipperfield and W. Feng, "Comment on: Stratospheric Ozone Depletion at Northern Mid-Latitudes in the 21st Century: The Importance of Future Concentrations of Greenhouse Gases Nitrous Oxide and Methane," Geophys. Rev. Lett. **30** (7), 42-1–42-4 (2003).
24. I. G. Dyominov and A. M. Zadorozhny, "The Numerical Simulation of Anthropogenic Impacts on the Ozonosphere," in *Proceedings of the 1st American–Soviet Meeting on Atmospheric Ozone* (Gidrometeoizdat, Moscow, 1989), pp. 186–217.
25. I. G. Dyominov, N. F. Elanskii, Yu. E. Ozolin, and V. K. Petukhov, "Estimation of the Effect of Energiya and Shuttle Regular Launches on the Ozone Layer and Climate of the Earth," Preprint No. 1, IFA RAN (Institute of Atmospheric Physics, Russian Academy of Sciences, 1992).
26. I. G. Dyominov, A. M. Zadorozhny, and N. F. Elansky, "Effects of NO_x and SO_2 Injections by Supersonic Aviation on Sulfate Aerosol and Ozone in the Troposphere and Stratosphere," in *Proceedings of the International Colloquium on Impact of Aircraft Emission upon the Atmosphere* (Paris, 1996), Vol. 2, pp. 595–600.
27. D. Weisenstein, M. K. W. Ko, I. G. Dyominov, *et al.*, "The Effects of Sulfur Emissions from HSCT Aircraft: A 2-D Model Intercomparison," J. Geophys. Res. D **103**, 1527–1547 (1998).
28. I. G. Dyominov, M. A. Merzliakov, and N. A. Vityugova, *Investigation of Global Influence of Nitrogen Oxides and Sulfur Dioxide Emission from Supersonic Aircraft on Ozone Layer and Aerosol Composition of Atmosphere*, Final Report on the NASA Research Grant NAG 5–3409 (Novosibirsk, 1999).
29. I. G. Dyominov and A. M. Zadorozhny, "Contribution of Solar UV Radiation to the Observed Ozone Variations during the 21st and 22nd Solar Cycles," Adv. Space Res. **27**, 1949–1954 (2001).
30. W. B. DeMore, S. P. Sander, D. M. Golden, *et al.*, *Chemical Kinetics and Photochemical Data for Use in Stratospheric Modeling, Evaluation Number 12*, (JPL Publication, 1997)
31. R. R. Garcia and S. Solomon, "A Numerical Model of the Zonally Averaged Dynamical and Chemical Structure of the Middle Atmosphere," J. Geophys. Res. C **88**, 1379–1400 (1983).
32. M. E. Van Hoosier, J.-D. F. Bartoe, G. E. Brueckner, and D. K. Prinz, "Absolute Solar Spectral Irradiance 120–400 nm (Results from the Solar Ultraviolet Spectral Irradiance Monitor-SUSIM-Experiment on Board Spacelab 2)," Astrophys. Lett. Commun. **27** (3), 163–168 (1988).
33. H. Neckel and D. Labs, "The Solar Radiation between 3300 and 12500 Å," Solar Phys. **90**, 205–258 (1984).
34. M. Y. Danilin and J. C. McConnell, "Heterogeneous Reactions in a Stratospheric Box Model: A Sensitivity Study," J. Geophys. Res. D **99**, 25681–25696 (1994).
35. D. R. Hanson and A. R. Ravishankara, "Reactive Uptake of $ClONO_2$ onto Sulfuric Acid Due to Reaction with HCl and H_2O," J. Phys. Chem. **98**, 5728–5735 (1994).
36. D. R. Hanson, A. R. Ravishancara, and S. Solomon, "Heterogeneous Reactions in Sulfuric Acid Aerosols: A Framework for Model Calculations," J. Geophys. Res. D **99**, 3615–3630 (1994).
37. M. Y. Danilin and J. C. McConnell, "Stratospheric Effects of Bromine Activation on/in Sulfate Aerosol," J. Geophys. Res. D **100**, 11237–11244 (1995).
38. D. R. Hanson, A. R. Ravishankara, and E. R. Lovejoy, "Reaction of $BrONO_2$ with H_2O on Submicron Sulfuric Acid Aerosol and the Implications for the Lower Stratosphere," J. Geophys. Res. D **101**, 9063–9069 (1996).
39. D. K. Weisenstein, G. K. Yue, M. K. W. Ko, *et al.*, "A Two-Dimensional Model of Sulfur Species and Aerosols," J. Geophys. Res. D **102**, 13019–13035 (1997).
40. I. G. Guterman, "Atmospheric Humidity Averaged over the Vertical and Latitude," Tr. VNIIGMI, No. 72, 3–12 (1980).
41. A. N. Oort, *Global Atmospheric Circulation Statistics, 1958–1973* (NOAA, Princeton, 1983).
42. M. K. W. Ko, H. R. Schueider, R.-L. Shia, *et al.,* "A Two-Dimensional Model with Coupled Dynamics, Radiation, and Photochemistry. 1. Simulation of the Middle Atmosphere," J. Geophys. Res. D **98**, 20429–20440 (1993).
43. M. J. Prather, "Numerical Advection by Conservation of Second-Order Moments," J. Geophys. Res. D **91**, 6671–6681 (1986).

44. Ya. I. Frenkel', *Kinetic Theory of Fluids* (Nauka, Leningrad, 1975) [in Russian].
45. P. Hamill, R. P. Turco, C. S. Kiang, *et al.*, "An Analysis of Various Nucleation Mechanisms for Sulfate Particles in the Stratosphere," J. Aerosol Sci. **13**, 561–585 (1982).
46. G. Pitari, V. Rizi, L. Ricciardulli, and G. Visconti, "High-Speed Civil Transport Impact: Role of Sulfate, Nitric Acid Trihydrate, and Ice Aerosols Studied with a Two-Dimensional Model Including Aerosol Physics," J. Geophys. Res. D **98**, 23141–23164 (1993).
47. R. P. Turco, P. Hamill, O. B. Toon, *et al.*, "A One-Dimensional Model Describing Aerosol Formation and Evolution in the Stratosphere, I. Physical Processes and Mathematical Analogs," J. Atmos. Sci. **36**, 699–717 (1979).
48. O. B. Toon, R. P. Turco, D. Westphal, *et al.*, "A Multidimensional Model for Aerosols: Description of Computational Analogs," J. Atmos. Sci. **45**, 2123–2143 (1988).
49. M. L. Asaturov, M. I. Budyko, K. Ya. Vinnikov, *et al.*, *Volcanoes, Stratospheric Aerosol, and the Earth's Climate* (Gidrometeoizdat, Leningrad, 1986) [in Russian].
50. A. A. Samarskii, *Introduction to the Theory of Difference Schemes* (Nauka, Moscow, 1971) [in Russian].
51. S.-C. S. Ou and K.-N. Liou, "A Two-Dimensional Radiation–Turbulence Climate Model. I: Sensitivity to Cirrus Radiative Properties," J. Atmos. Sci. **41**, 2289–2309 (1984).
52. I. G. Dyominov, "On the Influence of Variations in the Composition of Trace Gases on the Thermal Regime of the Ozonosphere," Opt. Atmos. **1** (9), 63–72 (1988).
53. T. Dunkerton, "On the Mean Meridional Mass Motions of the Stratosphere and Mesosphere," J. Atmos. Sci. **35**, 2325–2333 (1978).
54. J. Boyd, "The Noninteraction of Waves with Zonally Averaged Flow on Spherical Earth and Interrelationship of Eddy Fluxes of Energy Heat and Momentum," J. Atmos. Sci. **33**, 2285–2291 (1976).
55. G. Pitari and G. Visconti, "Two-Dimensional Tracer Transport: Derivation of Residual Mean Circulation and Eddy Transport Tensor from a 3-D Model Data Set," J. Geophys. Res. D **90**, 8019–8032 (1985).
56. *Scientific Assessment of Ozone Depletion: 1989*, WMO Global Ozone Research and Monitoring Project Report No. 20 (Geneva, 1989).
57. A. M. Zadorozhny, V. N. Kikhtenko, G. A. Kokin, *et al.*, "Middle Atmosphere Response to the Solar Proton Events of October 1989 Using the Results of Rocket Measurements," J. Geophys. Res. D **99**, 21059–21069 (1994).
58. T. Y. W. Huang and G. P. Brasseur, "Effect of Long-Term Solar Variability in a Two-Dimensional Interactive Model of the Middle Atmosphere," J. Geophys. Res. D **98**, 20413–20427 (1993).
59. G. J. Rottman, "Observation of Solar UV and EUV Variability," Adv. Space Res. **8** (7), 53–66 (1988).
60. *Scientific Assessment of Ozone Depletion: 1991*, WMO Global Ozone Research and Monitoring Project Report No. 25 (Geneva, 1992).
61. S. L. Baughcum and S. C. Henderson, *Aircraft Emission Inventories Projected in Year 2015 for a High-Speed Civil Transport (HSCT) Universal Airline Network*, NASA Contractor Report No. CR-4659 (NASA, Washington, DC, 1995).
62. M. P. McCormick and T. J. Swissler, "Stratospheric Aerosol Mass and Latitudinal Distribution of the El Chichon Eruption for October 1982," Geophys. Rev. Lett. **10**, 877–880 (1983).
63. J. F. Vedder, E. P. Condon, E. C. Inn, *et al.*, "Measurements of Stratospheric SO_2 after the El Chichon Eruptions," Geophys. Rev. Lett. **10**, 1045–1048 (1983).
64. D. J. Hofmann and J. M. Rosen, "On the Temporal Variation of Stratospheric Aerosol Size and Mass during the First 18 Months Following the 1982 Eruptions of El Chichon," J. Geophys. Res. **89**, 4883–4890 (1984).
65. G. J. Bluth, S. D. Doiron, C. C. Schnetzler, *et al.*, "Global Tracking of the SO_2 Clouds from the June 1991 Mount Pinatubo Eruptions," Geophys. Rev. Lett. **19**, 151–154 (1992).
66. M. P. McCormick and R. E. Veiga, "SAGE II Measurements of Early Pinatubo Aerosols," Geophys. Rev. Lett. **19**, 155–158 (1992).
67. X. Tie, X. Lin, and G. Brasseur, "Two-Dimensional Coupled Dynamical/Chemical/Microphysical Simulation of Global Distribution of El Chichon Volcanic Aerosols," J. Geophys. Res. D **99**, 16779–16792 (1994).
68. J. F. Gleason, P. K. Bhartia, J. R. Herman, *et al.*, "Record Low Global Ozone in 1992," Science **260** (5107), 523–526 (1993).

Translated by N. Tret'yakova